Suramin Affects Coupling of Rhodopsin to Transducin

Nicole Lehmann,* Gopala Krishna Aradhyam,† and Karim Fahmy*
*Institut für Molekulare Medizin und Zellforschung, Albert-Ludwigs-Universität, D-79104 Freiburg, Germany; and †Howard Hughes Medical Institute, Laboratory of Molecular Biology and Biochemistry, Rockefeller University, New York, New York 10021 USA

ABSTRACT Suramin, a polysulfonated naphthylurea, is under investigation for the treatment of several cancers. It interferes with signal transduction through G_s, G_i, and G_o, but structural and kinetic aspects of the molecular mechanism are not well understood. Here, we have investigated the influence of suramin on coupling of bovine rhodopsin to G_t, where G-protein activation and receptor structure can be monitored by spectroscopic in vitro assays. G_t fluorescence changes in response to rhodopsin-catalyzed nucleotide exchange reveal that suramin inhibits G_t activation by slowing down the rate of complex formation between metarhodopsin-II and G_t. The metarhodopsin-I/-II photoproduct equilibrium, GTPase activity, and nucleotide uptake by G_t are unaffected. Attenuated total reflection Fourier transform infrared spectroscopy shows that the structure of rhodopsin, metarhodopsin-II, and the metarhodopsin-II G_t complex is also not altered. Instead, suramin dissociates G_t from disk membranes in the dark, whereas metarhodopsin-II G_t complexes are stable. Förster resonance energy transfer suggests a suramin-binding site near Trp^{207} on the $G_{t\alpha}$ subunit ($K_d \sim 0.5\ \mu M$). The kinetic analyses and the structural data are consistent with a specific perturbation by suramin of the membrane attachment site on $G_{t\alpha}$. Disruption of membrane anchoring may contribute to some of the effects of suramin exerted on other G-proteins.

INTRODUCTION

Suramin, a hexasulfonated polyaromatic naphthylurea (1.4 kDa), is under study for therapeutic activity in phase II trials in the treatment of several cancers (Mirza et al., 1997; Dawson et al., 1998; Dreicer et al., 1999). It exhibits antiangiogenetic and antiproliferative activity (Firsching et al., 1995) by interfering with the binding of several growth factors to their receptors (Coffey et al., 1987). These properties can be enhanced in suramin analogs (Gagliardi et al., 1998). However, adverse effects of suramin are dose-limiting (Chaudhry et al., 1996), and the molecular basis of its action is not well understood. The function of several cellular signaling proteins, such as protein-tyrosine phosphatases (Zhang et al., 1998) and protein kinase C (Khaled et al., 1995) is perturbed, and recent interest in suramin focuses on its ability to interfere also with signaling through G-protein-coupled receptors (GPCRs). GPCRs are heptahelical transmembrane proteins that respond to extracellular signals, such as binding of a hormone or a neurotransmitter, by catalyzing GDP/GTP exchange in cytosolic guanosine-nucleotide-binding proteins (G-proteins) (for reviews see Ji et al., 1998; Gether, 2000). Suramin has been shown to uncouple α_2- and β_2-adrenergic receptors from G_i and G_s, respectively (Huang et al., 1990). It has also been shown that suramin inhibits activation of pertussis-toxin-sensitive G-proteins by δ-opioid receptors in NG 108–15 cell membranes, whereas nucleotide exchange induced by serum factors binding to an unidentified receptor was not affected (Butler et al., 1988). Based on these initial observations, the potential of suramin analogs to interfere with signaling by different receptor G-protein tandems has been investigated systematically. A suramin analog has been described that uncouples A_1 adenosine and D_2 dopamine receptors from G_i/G_o with different specificity (Beindl et al., 1996; Waldhoer et al., 1998), and a number of analogs have been synthesized that act as subtype-specific G-protein inhibitors (Hohenegger et al., 1998; Waldhoer et al., 1998). Such studies emphasize the role of G-proteins as potential drug targets (Höller et al., 1999). However, details of the molecular mechanism by which suramin affects structural and kinetic parameters of receptor G-protein interactions remain to be elucidated. In an attempt to exploit a well characterized in vitro model system for GPCR signaling, we have investigated the effect of suramin on activation of transducin (G_t) by the bovine photoreceptor rhodopsin. For this system, biophysical assays for conformational changes of the receptor, G_t binding, and G_t activation are available. Based on the homology of class I (rhodopsin-like) GPCRs, a study of the action of suramin on rhodopsin G_t interactions helps to identify molecular mechanisms by which the drug may affect signaling in related systems.

Rhodopsin is a prototypical GPCR (Helmreich and Hofmann, 1996; Menon et al., 2001; Okada et al., 2001) and the only one for which a crystal structure has been solved (Palczewski et al., 2000). Rhodopsin is unique as it is not ligand-activated. Instead, 11-*cis*-retinal is covalently attached to Lys^{296} of the apoprotein via a protonated Schiff base (Oseroff and Callender, 1974). Photoisomerization to all-*trans*-retinal promotes structural changes involving helix-helix interactions and rigid body movements (Farrens et al., 1996; Han et al., 1996; Sheikh et al., 1996). As a consequence, cytosolic domains of the active metarhodopsin-II (MII) state bind G_t and catalyze GDP/GTP exchange.

Submitted July 26, 2001, and accepted for publication October 1, 2001.

Address reprint requests to Dr. Karim Fahmy, Institut für Molekulare Medizin und Zellforschung, Universität Freiburg, Albertstrasse 23, D-79104 Freiburg, Germany. Tel.: 49-761-203-5380; Fax: 49-761-203-2921; E-mail: fahmy@uni-freiburg.de.

0006-3495/02/02/793/10 $2.00

Signaling by the rhodopsin G_t tandem has been optimized for maximal light sensitivity, which implies minimization of dark noise (Birge and Barlow, 1995; Rieke and Baylor, 1996). Correspondingly, basal nucleotide exchange, typical of other G-proteins, is negligible in G_t. The unique features of rhodopsin and G_t suggest that interference with receptor coupling is the predominant mode of action by which a pharmacologically active substance may modulate G_t activation. Other potential perturbations such as interference with basal G-protein activation or competition with agonist binding are not expected to contribute to the readout from this model system.

We have applied fluorescence spectroscopy to analyze binding of suramin to $G_{t\alpha}$ and to monitor rhodopsin-catalyzed G_t activation. By attenuated total reflection (ATR) Fourier transform infrared (FTIR) spectroscopy we have investigated the influence of suramin on the structure of rhodopsin and the $MIIG_t$ complex. We show that suramin binds to $G_{t\alpha}$ but does not affect either GTP uptake or GTPase activity. Likewise, structural changes during rhodopsin activation are not influenced. Instead, the rate of $MIIG_t$ formation is reduced by a dose-dependent inhibition of membrane anchoring of G_t. In addition to inferences on receptor G-protein coupling in nonvisual signaling, the data are relevant for the molecular characterization of side effects on vision in patients receiving suramin treatment. A variety of ocular symptoms have been described (for example, Hemady et al., 1996).

MATERIALS AND METHODS

Purification of rhodopsin and transducin

Preparation of washed membranes from bovine rod outer segments (ROSs) was carried out as described (Papermaster, 1982) with minor modifications. G_t was purified from illuminated, osmotically shocked ROSs by successive washes and hexyl agarose chromatography (Kühn, 1980; Fung et al., 1981). G_t was eluted with 300 mM NaCl in buffer solution (10 mM sodium phosphate, pH 7.2, 2 mM $MgCl_2$, 1 mM dithiothreitol (DTT), 0.1 mM phenylmethylsulfonyl fluoride). Pooled fractions were diluted with buffer to a final concentration of 100 mM NaCl. $G_{t\beta\gamma}$ and $G_{t\alpha}$ were isolated from G_t (prepared from bovine retinas, Lawson, Lincoln, NE) according to published methods (Shichi et al., 1984) using a Hitachi LC-organizer high-performance liquid chromatography system with 1 ml of Hi-Trap Blue Sepharose column (Amersham Pharmacia Biotech, Piscataway, NJ). The proteins were eluted with a 0–2 M NaCl gradient. Protein concentrations were determined using the Bio-Rad protein assay reagent according to manufacturer's instructions. The subunits were stored at −20°C in a 50% glycerol buffer until use.

ATR-FTIR spectroscopy

Disk membranes (1–2 nmol of rhodopsin) were dried under nitrogen on a trapezoidal (45°) internal reflection element (IRE) made of ZnSe (3.5 cm^2) mounted in a Bruker A737 temperature-controlled dialysis-coupled (10,000 MW cutoff) ATR cell. Under these conditions, membrane stacks of at least 50 layers are expected to form, when the surface coverage by rhodopsin in disk membranes is estimated from the crystal structure (Palczewski et al., 2000) to be ~1500 $Å^2$. Thus, more than 98% of rhodopsin is excluded from possible denaturing influences of the ZnSe surface and the functionality (normal light-dependent MII formation and G_t activation) of the resulting matrix of immobilized disk membranes has been demonstrated (Fahmy, 1998).

After addition of G_t (0.5–1 ml, 4–6 μM, 10 mM sodium phosphate buffer, pH 7.2, 100 mM NaCl, 2 mM $MgCl_2$, 1 mM DTT) to the sample compartment, its association with disk membranes was monitored in a vector 22 FTIR spectrophotometer (Bruker, Karlsruhe, Germany). GTP, suramin, and heparin were purchased from Sigma-Aldrich (Milwaukee, WI) and used without further purification. Dissociation of G_t from disk membranes was induced by addition of the appropriate amounts of these substances to the dialysis reservoir of the ATR cell. Subsequent spectral changes were measured as the difference between the absorption (calculated from 256 interferograms) at a given time after and the absorption immediately before the addition of either substance. Experiments were carried out at 17°C. Light-induced IR absorption changes during metarhodopsin II (MII) formation in the absence of G_t were measured at 10°C (10 mM sodium phosphate buffer, pH 5, 100 mM NaCl, 30 s illumination with 150-W projector light using a GG 495 filter from Schott, (Mainz, Germany).

Fluorescence measurements

GTP-induced changes of tryptophan fluorescence from G_t were recorded with a home-built instrument, using fiber optics attached to a temperature-controlled cuvette holder for excitation and emission in 90° geometry. Excitation was achieved with UV light from a deuterium lamp equipped with an interference filter transmitting 290–310-nm light (300FS10–25, L.O.T. Oriel, Darmstadt, Germany). Emitted light (λ_{max} = 345 nm) was detected by a photomultiplier after transmission through a 335-nm cutoff filter (WG 335 Schott). Integration time of the fluorescence signals was 4 s and the reaction mixture was continuously stirred by a magnetic stir bar in a quartz cuvette. A suspension of disk membranes in buffer containing 1–2 μM G_t was photoactivated 5 min before starting fluorescence recordings. The reaction mixture (0.8 ml) was thermostatted to 27°C.

FRET from suramin to $G_{t\alpha}$ was measured in a Spex Fluorolog 3–11 τ3 spectrofluorometer equipped with a 450-W xenon arc lamp. Excitation was at 295 nm, and emission was recorded between 315 and 450 nm. The fluorescence spectra were recorded in 10 mM Tris buffer (pH 7.2), 100 mM NaCl, 2 mM $MgCl_2$, 1 mM DTT, 5 μM GDP, and 0.01% dodecyl maltoside.

Data analysis

Kinetic fluorescence data were fitted by numerical integration of rate equations using the Newton method. In a two-step reaction model, the time derivative of the concentration of the GTP-bound state of G_t was assumed to depend on the rate constants k_1 and k_2, describing formation of $G_{t\alpha}$(GTP) from $G_{t\alpha}$(GDP) and GTP (catalyzed by MII) and decay of $G_{t\alpha}$(GTP) to $G_{t\alpha}$(GDP) and P_i by intrinsic GTPase activity of $G_{t\alpha}$, respectively:

$$d[G_{t\alpha}(GTP)]/dt = k_1 \times [G_{t\alpha}(GDP)] \times [GTP] - k_2 \times [G_{t\alpha}(GTP)] \quad (1)$$

Microscopic rate constants for the formation of $MIIG_t$ as well as for GDP release were not explicitly included. Instead, the concentration of $MIIG_t$ was implicitly defined in proportion to the concentration of $G_{t\alpha}$(GDP).

In a more realistic three-step model, the formation of the $MIIG_t$ complex from MII and G_t(GDP) and uptake of GTP (followed by immediate

dissociation of the $MIIG_t$ complex) was described by the rate constants k_c and k_u, respectively:

$$d[MIIG_t]/dt = k_c \times [MII] \times [G_{t\alpha}(GDP)] - k_u \times [MIIG_t] \times [GTP] \quad (2)$$

$$d[G_{t\alpha}(GTP)]/dt = k_u \times [MIIG_t] \times [GTP] - k_h \times [G_{t\alpha}(GTP)], \quad (3)$$

where k_h is the rate constant for GTP hydrolysis. In contrast to the two-step model, the rate of $MIIG_t$ formation, rather than its concentration, is proportional to the concentration of $G_{t\alpha}(GDP)$ in the three-step model. This leads to a superior simulation when $MIIG_t$ formation becomes rate limiting.

Data on FRET from $G_{t\alpha}$ to suramin were analyzed to determine the fraction $f(G_{t\alpha})$ of free $G_{t\alpha}$ in the presence of varying amounts of suramin according to Eq. 4:

$$f(G_{t\alpha}) = (F_S - F_q)/(F_0 - F_q), \quad (4)$$

where F_s, F_q, and F_0 is the tryptophan fluorescence in the presence of a given suramin concentration, at maximal concentration of suramin, and in the absence of suramin, respectively. The right side of Eq. 4 was determined from peak emission values at 343 nm. These were corrected for inner filtering by suramin absorption at the excitation and emission wavelength as described (Pigault and Gérard, 1984) using absorption coefficients of 20,500 and 9,440 M^{-1} cm^{-1} at 295 and 343 nm, respectively. Absorption and fluorescence spectra of suramin have been published (Mély et al., 1997; Zhang et al., 1998).

RESULTS

Fluorescence monitoring of G_t activation

To investigate the action of suramin on receptor-dependent G-protein signaling, we have designed experiments using the bovine photoreceptor rhodopsin and G_t as a model system. Rhodopsin-catalyzed nucleotide exchange and GTP hydrolysis by G_t were monitored with a real-time G_t activation assay (Fahmy and Sakmar, 1993; Ernst et al., 2000) based on intrinsic G-protein fluorescence (Higashijima et al., 1987). The fluorescence increases of Trp^{207} of $G_{t\alpha}(GTP)$ or $G_{t\alpha}(GTP\gamma S)$ versus $G_{t\alpha}(GDP)$ (Faurobert et al., 1993) allow the observation of nucleotide uptake and hydrolysis during multiple cycles of G_t activation. Fig. 1 shows fluorescence recordings from G_t in a suspension of light-activated disk membranes. Repeated addition of GTP caused transient fluorescence increases corresponding to the increase of $[G_{t\alpha}(GTP)]$ followed by a decrease due to GTPase activity of $G_{t\alpha}$. The traces evidence the catalytical nature of the G_t turnover and the stability of rhodopsin G_t interactions during the time of the experiment. Addition of a saturating amount of the nonhydrolyzable GTP analog GTPγS caused a persistent fluorescence increase. The decrease in fluorescence upon further addition of GTPγS as well as the fluorescence signal reached at the end of GTP-induced signals scaled precisely with the corresponding dilution of the reaction buffer.

The described assay allows an accurate evaluation of the kinetics of rhodopsin G_t coupling. The peak height and

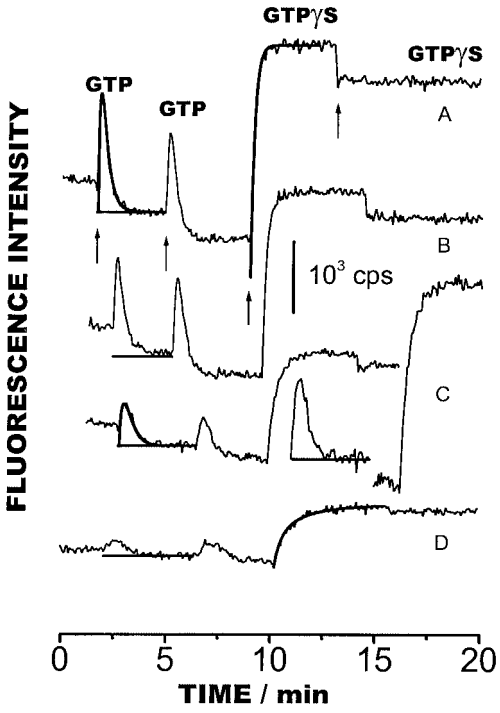

FIGURE 1 Influence of suramin on nucleotide-dependent fluorescence changes of $G_{t\alpha}$ ($[GTP] < [G_t]$). Arrows indicate injection of GTP (1.4 μM) and GTPγS (6 μM) to a reaction mixture (10 mM sodium phosphate, pH 7.2, 100 mM NaCl, 2 mM $MgCl_2$, 1 mM DTT) containing photoactivated rhodopsin (150 nM) in suspension of disk membranes and freshly prepared G_t (1.8 μM). Experiments were carried out at 27°C. Bars delimit identical areas under each trace when normalized to the size of the respective GTPγS-induced fluorescence increase. (*A*) Fluorescence signals in the absence of suramin. The curve drawn through the first GTP-induced signal was calculated according to Eq. 1 with $k_1 = 0.147$ $\mu M^{-1}s^{-1}$ and $k_2 = 0.059$ s^{-1}. For the simulation of the GTPγS-induced signal, k_2 was set to zero. (*B*) Fluorescence signals at 3 μM suramin (initial fluorescence 90% of that in *A*). (*C*) Fluorescence signals at 12 μM suramin (initial fluorescence 67% of that in *A*). The first GTP-induced signal has been fitted according to Eq. 1 with $k_1 = 0.100$ s^{-1} and $k_2 = 0.058$ s^{-1}. The same transient as well as the GTPγS-induced signal was replotted to the right in a scale in which the GTPγS-induced signal is normalized to that in *A*, to better appreciate the normalized peak area of the GTP-induced signal (see text for details). (*D*) Fluorescence signals at 24 μM suramin (initial fluorescence 50% of that in *A*). The curve drawn through the GTPγS-induced signal was calculated as in *A*, but k_1 was reduced by a factor of 0.14 ($k_2 = 0.0$ s^{-1}).

width of the GTP-induced transients is determined by the apparent rate of the rising and falling phase of $[G_{t\alpha}(GTP)]$. The peak height (normalized to the GTPγS-induced signal) decreased whereas the peak width increased as a function of suramin concentration. This indicates that suramin caused an increase of the apparent fluorescence rise time. In principle, the effect of suramin may be accounted for by denaturing G_t or rhodopsin. However, the more thorough quantitative analysis of reaction kinetics as well as spectroscopic data, presented below, strongly suggest that the data in Fig. 1 must be explained by a specific inhibitory effect of suramin on the MII-dependent formation of $G_{t\alpha}(GTP)$.

For a given rate of GTP hydrolysis, the area under the transient fluorescence signal is a measure of the amount of GTP hydrolyzed. Because identical aliquots of GTP were injected in all experiments, the peak area is not expected to depend on the presence of suramin if the drug exclusively influenced the formation of $MIIG_t$. Integration intervals and baseline positions for GTP-induced peaks are represented by the length and vertical position, respectively, of the bars in Fig. 1. In trace *A*, the baseline was determined by the fluorescence level at the end of the transient. In traces *B–D*, baselines were adjusted to obtain identical normalized peak areas as in trace *A*. The correspondence of normalized areas under GTP-induced signals is exemplified in panel *C*, where the GTP-induced transient has been replotted in a scale in which the GTPγS-induced signal (shown to the right) matches that in *A*. Evidently, the criterion of invariant peak areas yields excellent agreement with the measured traces. Thus, an effect of suramin on GTPase activity is negligible within the accuracy of the experiment.

Estimates of the apparent rate constants k_1 and k_2 for GTP uptake and hydrolysis, respectively, can be obtained in the realm of a two-step reaction model described by Eq. 1. The larger k_1/k_2, the higher is the fluorescence peak. For each peak, k_1/k_2 assumes well defined values that were used to generate the curves drawn through the data in Fig. 1. All fluorescence traces are well described by the two-step model. The influence of suramin can be accounted for by a successive reduction of k_1 at a constant value of k_2. This agrees with the model-independent evaluation of peak areas. At all suramin concentrations tested, the data could be fitted with hydrolysis rates of $0.044\ s^{-1} < k_2 < 0.059\ s^{-1}$, which is in agreement with the range of reported hydrolysis rates (Yamanaka et al., 1985; Antonny et al., 1993; Otto-Bruc et al., 1994) and renders unlikely denaturation of G_t by suramin. In contrast, k_1 had to be reduced by factors of 0.85, 0.52, 0.38, and 0.14 in the presence of 3, 6, 12, and 24 μM suramin, respectively, relative to its value in the absence of suramin. Therefore, a pronounced influence is exerted on the reaction(s) that lead to uptake of GTP by G_t, whereas an effect of suramin on GTP hydrolysis (k_2) must be small, if it is present at all. The drop in k_1 for G_t activation with GTPγS ($k_2 = 0$) parallels that for activation with GTP. For example, the GTPγS-induced signal at 24 μM suramin (Fig. 1 *D*) is approximated by the model when k_1 is reduced by the same factor (0.14) that was used for the simulation of the GTP-induced signal.

In the measurements shown in Fig. 1, where [GTP] < $[G_t]$, the reaction mixture had become depleted of GTP before a steady state was reached during which GTP hydrolysis can approximately balance the formation of $G_{t\alpha}$(GTP). At higher [GTP], a nearly constant fraction of $G_{t\alpha}$(GTP) was present before the pool of nucleotide was eventually turned over. This resulted in a broadening of the fluorescence signal that cannot be reproduced by the two-step reaction model. Fluorescence time courses with [GTP] > $[G_t]$ (Fig. 2) were analyzed in a more realistic model (Eqs. 2 and 3) to assess specifically the influence of suramin on $MIIG_t$ formation (k_c) and GTP uptake (k_u). The values for k_u and k_h in the absence of suramin were held constant and only k_c was varied. In an iterative process, a pair of rate constants k_u and k_h was found that allowed simultaneous fits of reasonable quality to all traces. At constant rates of k_u of $0.14\ \mu M^{-1}\ s^{-1}$ and k_h of $0.031\ s^{-1}$, k_c was reduced by factors of 0.43, 0.3, and 0.12 at 2.5, 5.0, and 10.0 μM suramin, respectively, relative to its value of $0.7\ \mu M^{-1}\ s^{-1}$ in the absence of suramin. [GTP] was increased by 18% at 10 μM suramin (Fig. 2 *D*) to extend the steady state during which [$G_{t\alpha}$(GTP)] was only slowly changing. In contrast to the two-step model, the three-step model is clearly able to

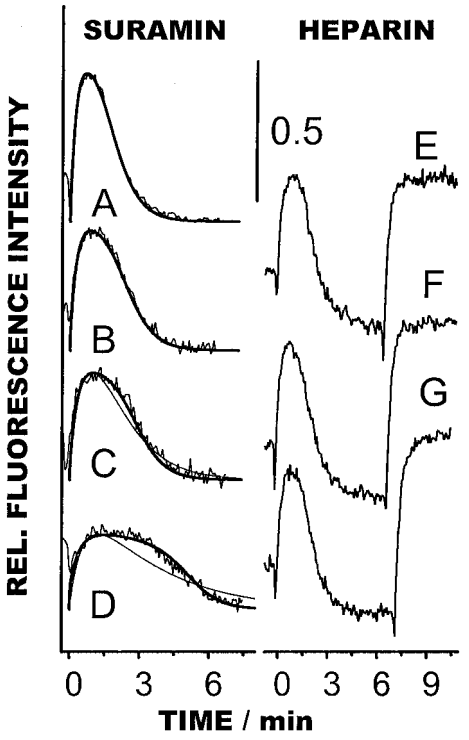

FIGURE 2 Influence of suramin on nucleotide-dependent fluorescence changes of $G_{t\alpha}$ ([GTP] > $[G_t]$). Injection of GTP (2.5 μM (*A–C*), 3.1 μM (*D*)) to a reaction mixture containing photoactivated rhodopsin (130 nM) in suspension of disk membranes and freshly prepared G_t (1 μM). Experimental conditions are as given in Fig. 1. The scale bar corresponds to 50% of the GTPγS-induced signal. (*A–D*) Fluorescence signals in the absence and presence of 2.5, 5.0, and 10.0 μM suramin, respectively. Solid lines are numerical solutions of rate equations (Eqs. 2 and 3) using $k_u = 0.14\ \mu M^{-1}s^{-1}$ and k_h of $0.031\ s^{-1}$ for all traces, whereas k_c was reduced by factors of 0.43, 0.3, and 0.12 relative to its value of $0.7\ \mu M^{-1}s^{-1}$ in the absence of suramin. Additional thin lines in traces *C* and *D* are results from simulations in which k_c and k_h were fixed (at $0.7\ \mu M^{-1}s^{-1}$ and $0.031\ s^{-1}$, respectively) at both suramin concentrations, whereas k_u was $0.06\ \mu M^{-1}s^{-1}$ and $0.026\ \mu M^{-1}s^{-1}$ at 5 and 10 μM suramin, respectively. (*E–G*) Fluorescence changes induced by injection of GTP (2.5 μM) followed by GTPγS (6 μM) in the presence of heparin (7.5, 15.0, and 30.0 mg/L, respectively) measured in parallel with traces *B–D* in reaction mixtures made from identical stocks.

describe this situation. The rate constants for $MIIG_t$ association and GTP hydrolysis in the absence of suramin are of the correct magnitude (Schleicher and Hofmann, 1987; Yamanaka et al., 1985; Antonny et al., 1993; Otto-Bruc et al., 1994), and we conclude that suramin acts primarily on k_c. The additional curves in Fig. 2, *C* and *D* (thin lines) were obtained by exclusively adjusting k_u. Obviously, the shape of the resulting time courses is incorrectly described, particularly at high suramin concentrations. This supports a specific action of suramin on $MIIG_t$ formation while other molecular processes on the G_t activation/deactivation pathway can proceed normally. In control experiments (Fig. 2, *E–G*) in which heparin was substituted for suramin, the fluorescence changes were not affected, ruling out a general polyanionic effect on G_t activation. In summary, the kinetic analyses reveal that suramin slows down the light-dependent activation of G_t by reducing the rate of $MIIG_t$ complex formation, whereas GTP uptake and GTP hydrolysis is not affected.

Fluorescence energy transfer from $G_{t\alpha}$ to suramin

The reduction of both basal G_t fluorescence and the GTPγS-induced fluorescence increase indicates that suramin binds to $G_{t\alpha}$, thereby quenching its tryptophan fluorescence. The nucleotide-dependent fluorescence change of Trp^{207} was more affected than basal fluorescence. For example, basal fluorescence at 24 μM suramin was reduced by 50%, whereas the GTPγS-induced fluorescence change was reduced by 70% (Fig. 1, *A* and *D*). Quenching of $G_{t\alpha}$ fluorescence was further analyzed by fluorescence emission spectroscopy. When excited at 295 nm, $G_{t\alpha}$ fluorescence is maximal at 343 nm. With increasing suramin concentration, fluorescence at this wavelength decreased while emission from suramin above 400 nm increased (Fig. 3 *A*). At low suramin concentrations and 240 nM $G_{t\alpha}$, appearance of suramin fluorescence was barely visible, whereas an isosbestic point formed at 377 nm at suramin concentrations above 0.5 μM. The spectra indicate that $G_{t\alpha}$ and suramin form a donor-acceptor pair undergoing FRET with spectral features almost identical with those described for other suramin-binding proteins (Mély et al., 1997; Zhang et al., 1998). At 480 nM $G_{t\alpha}$, formation of an isosbestic point at 416 nm for suramin concentrations below 0.5 μM was reproducibly observed (Fig. 3 *B*). The decrease of $G_{t\alpha}$ fluorescence between 10 and 53 μM suramin and the concomitant increase of suramin fluorescence above 400 nm suggest that suramin binds to $G_{t\alpha}$ with a $K_d > 10$ μM. However, the insets in Fig. 3 show that the fraction of free $G_{t\alpha}$ (Eq. 4) was barely changing above 5 μM suramin when corrected for absorption of excitation and emission light by suramin (see Materials and Methods). The corrected data reveal that suramin binds to $G_{t\alpha}$ with a K_d of ~0.5 μM, typical of suramin binding to other G-proteins (Freissmuth et al., 1996). The fluorescence increase above 400 nm observed between 10 and 53 μM suramin was thus due to free suramin, and the decrease of tryptophan emission was caused by absorption of excitation light by suramin. This was expected as the amount of suramin exceeded that of $G_{t\alpha}$ by a factor of 40–200, implying preponderance of free suramin. Likewise, the upshift of the apparent isosbestic point at [suramin] > 0.5 μM from 377 nm to 390 nm at 240 and 480 nM $G_{t\alpha}$, respectively, is entirely consistent with stronger tryptophan emission bands in Fig. 3 *B* versus *A* superimposed with directly excited fluorescence from free suramin.

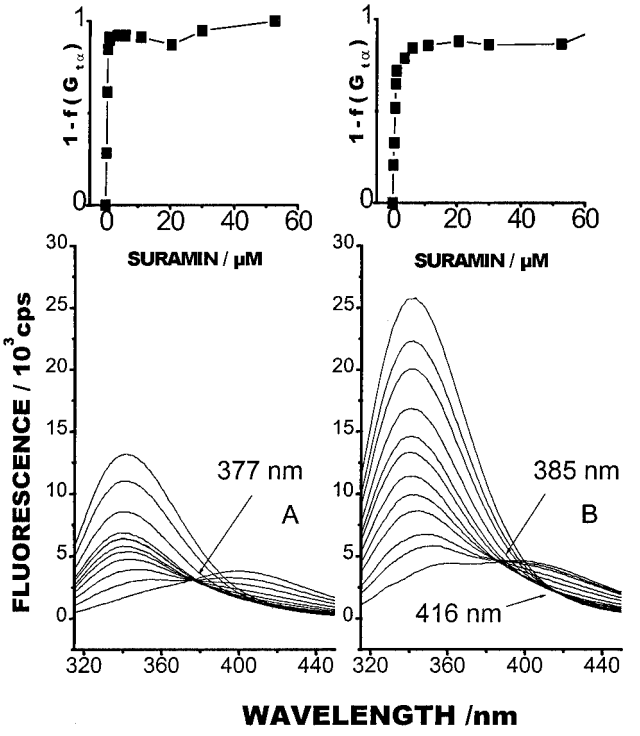

FIGURE 3 Förster resonance energy transfer from $G_{t\alpha}$ to suramin. Solutions of purified $G_{t\alpha}$ (10 mM Tris, pH 7.2, 100 mM NaCl, 2 mM $MgCl_2$, 1 mM DTT, 5 μM GDP) were excited at 295 nm and emission measured from 315 to 450 nm. (*A* and *B*) $G_{t\alpha}$ concentration was 240 and 480 nM, respectively. Suramin concentrations (from *top* to *bottom*) were 0.0, 0.25, 0.5, 0.74, 0.99, 1.23, 3.70, 6.14, 11.00, 20.58, 29.98, and 52.69 μM. Insets show the saturation of fluorescence quenching corrected for inner filtering by suramin (Materials and Methods) and for dilution (<13%) upon consecutive addition of aliquots from suramin stock solutions. Experiments were carried out at 27°C.

Influence of suramin on the structure of rhodopsin, MII, and $MIIG_t$ and on membrane anchoring of G_t

In addition to binding to $G_{t\alpha}$, reduced G_t activation may be caused by suramin shifting the MI/MII equilibrium toward the inactive MI species. However, UV-visible absorption changes did not show an absorption increase in the 460–

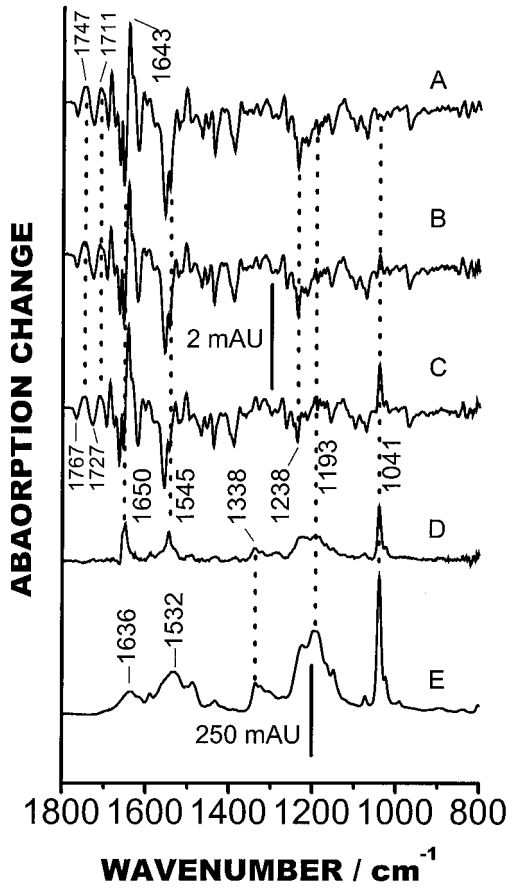

FIGURE 4 Light-induced ATR-FTIR spectra of rhodopsin. (*A–C*) Absorption changes typical of MII formation in the absence of suramin and at 50 and 500 μM suramin, respectively. Photoproduct bands show upwards, and absorption bands of the dark state are negative. Experiments were carried out at 10°C in buffer (10 mM sodium phosphate, pH 5, 100 mM NaCl) with disk membranes adsorbed on an IRE made of ZnSe. (*D*) Suramin-induced spectral changes in the MII difference spectra obtained by subtraction of trace *A* from trace *C*. (*E*) Infrared absorption of 60 mM suramin in H_2O, measured by ATR-FTIR.

480-nm range (MI) at the expense of decreased 380-nm absorption (MII, not shown). We have addressed more subtle effects of suramin on the conformation of rhodopsin, MII, and $MIIG_t$ by ATR-FTIR spectroscopy. Light-induced conformational changes in rhodopsin are accompanied by characteristic shifts in the frequencies of vibrational modes of the structurally affected parts of the protein backbone, amino acid side chains, and the retinal chromophore as reviewed in Siebert (1995). Consequently, light-induced FTIR difference spectra allow the detection of perturbations of the normal structural changes during MII formation. In contrast to transmissive FTIR spectroscopy, the ATR-FTIR technique applied here monitors absorption changes of disk membranes adsorbed on an internal reflection element (IRE) in the presence of a bulk aqueous phase. In addition to structural changes, shifts in the binding equilibrium between G_t or suramin in the aqueous phase and in disk membranes give rise to IR-absorption changes as the amount of absorbing species in the evanescent field of the IRE (extending ~1 μm from its surface) is affected. IR absorption changes during MII formation at pH 5 are shown in Fig. 4 (negative bands are caused by the dark state, and positive bands correspond to absorption by MII). Except for a small additional positive band at 1040 cm^{-1}, typical of suramin (Fig. 4 *E*), no alterations were observed in the difference spectrum recorded at 50 μM suramin (Fig. 4 *B*) versus normal MII formation (Fig. 4 *A*), although GTP-induced fluorescence signals were completely abolished at this concentration. At 500 μM suramin (Fig. 4 *C*), the light-induced absorption increase at 1040 cm^{-1} was larger, and additional alterations occurred in the amide I and II spectral range. These were identified by subtracting the normal MII difference spectrum from that measured in the presence of 500 μM suramin, resulting in the spectrum shown in Fig. 4 *D*. The flat baseline obtained between 1700 and 1800 cm^{-1} demonstrates that the C═O stretching vibrations of Asp^{83} (1767(−)/1747(+)), Glu^{113} (1711(+)), and Glu^{122} (1727(−)/1747(+)) (Fahmy et al., 1993; Rath et al., 1993; Jäger et al., 1994) were not altered. This confirms that the reduction of G_t activation cannot be attributed to a stabilizing effect of suramin on the MI state. A shift in the MI/MII equilibrium would have led to residual bands between 1700 and 1800 cm^{-1} (Fahmy, 1998) caused by protonated Glu^{122} and by protonation of Glu^{113} in MII. The absorption at 1040 cm^{-1} and the bands between 1400 and 1000 cm^{-1} correspond well with absorption by free suramin (Fig. 4 *E*) and indicate binding of suramin to photoactivated disk membranes. The alterations at 1650 and 1545 cm^{-1} may indicate an effect on the structure of dark rhodopsin at 500 μM suramin (i.e., in excess of serum concentrations of suramin in patients (Chaudhry et al., 1996)); however, the band at 1643 cm^{-1}, typical of the G_t activating conformation of MII (Fahmy et al., 1994; Zvyaga et al., 1996), was not affected. In conclusion, the FTIR difference spectra argue against structural perturbations of rhodopsin or MII by suramin in the low micromolar range.

To study the influence of suramin on the structure of $MIIG_t$, G_t was added to disk membranes in the dark. Binding of G_t is accompanied by characteristic absorption increases in the amide I (1610–1700 cm^{-1}) and II (1510–1580 cm^{-1}) frequency range (Fig. 5 *A*) as G_t accumulates in the evanescent field of the IRE. The functionality of MII G_t interactions under the conditions of the ATR-FTIR experiment has been demonstrated (Fahmy, 1998). After illumination, suramin was added by dialysis and ensuing absorption changes were recorded. Appearance of the drug in the evanescent field was evidenced by the sharp absorption increase at 1040 cm^{-1} (Fig. 5 *B*). In the amide I and II frequency range, slight absorption increases were observed as well and may have been caused by the amide groups in suramin or additional binding of G_t. More importantly, no negative bands occurred. Such bands are expected when

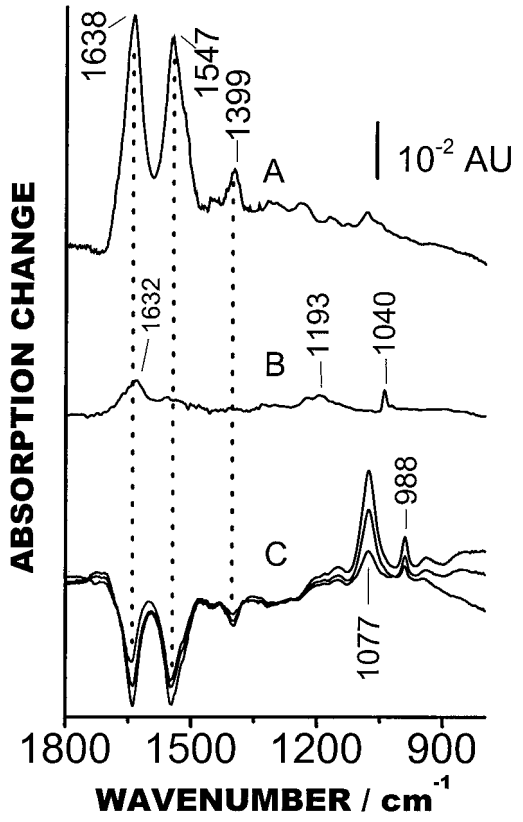

FIGURE 5 ATR-FTIR spectra induced by suramin and GTPγS in G_t-loaded disk membranes in the light. (*A*) Binding of G_t (10 mM sodium phosphate, pH 7.2, 150 mM NaCl, 2 mM $MgCl_2$, 1 mM DTT) in the dark to disk membranes. (*B*) Spectral changes accompanying dialysis of 30 μM suramin into the sample compartment after illumination (30 s with 150-W slide projector through GG495 Schott filter). (*C*) Spectral changes evoked by dialysis over 2, 5, and 15 min of 500 μM GTPγS and 20 mM sodium phosphate into the sample compartment. Spectral changes were calculated with respect to reference spectra recorded immediately before buffer exchange in the dialysis compartment. Experiments were carried out at 17°C.

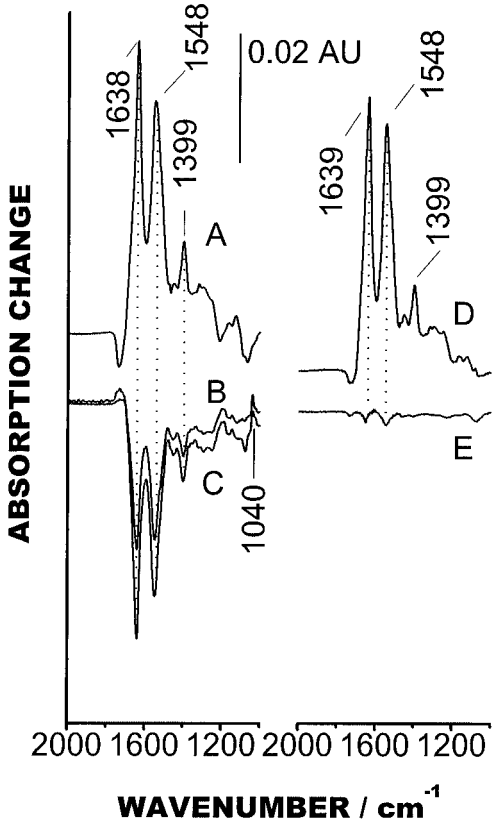

FIGURE 6 ATR-FTIR spectral changes during association of G_t with disk membranes in the dark followed by suramin-induced dissociation. (*A*) Absorption increase after binding of G_t to disk membranes in the dark. (*B*) and (*C*) Absorption decrease induced by dissociation of G_t from membranes upon dialysis of 20 and 100 μM suramin, respectively, into the sample compartment. (*D*) Binding of G_t to disk membranes in an independent experiment. (*E*) Absorption changes during subsequent dialysis of 3-kDA heparin (100 μM) into the sample compartment. Experimental conditions as given in Fig. 5.

suramin caused denaturation of $MIIG_t$, thereby shifting vibrational frequencies of structurally affected peptide bonds. If suramin causes conformational changes in $MIIG_t$ at all, they must be smaller than those accompanying the light-dependent formation of MII or $MIIG_t$, as these would clearly be visible as sharp superimposed difference bands of 1–3 mAU in the amide I/II range (Fahmy, 1998). Likewise, suramin does not dissociate $MIIG_t$. As shown in Fig. 5 *C*, dissociation of $MIIG_t$ upon addition of nucleotide is not prevented either. GTPγS was added to the dialysis compartment in a higher concentrated sodium phosphate buffer, providing a monitor of the buffer exchange by the absorption increase of inorganic phosphate at 1077 and 988 cm^{-1}. The loss of amide absorption of G_t coincided with the onset of absorption by inorganic phosphate, indicating that G_t dissociated from disk membranes with the arrival of the GTPγS-containing buffer in the evanescent field. The ATR-FTIR results suggest that the reduction of the apparent rate of $G_{t\alpha}$(GTP) formation as determined by the G_t activation assay is caused neither by a shift in MI/MII equilibrium nor by altered structures of MII/$MIIG_t$, nor by occupation of the GTP-binding site by suramin.

To test the influence of suramin on steps before $MIIG_t$ formation, G_t was allowed to bind to disk membranes in the dark (Fig. 6 *A*) and suramin was added without prior photoactivation. With the arrival of suramin in the evanescent field (1040 cm^{-1} absorption increase) amide I and II absorption of G_t decreased. This demonstrates that suramin promoted dissociation of G_t from disk membranes. At 20 μM and 100 μM suramin, ~60% and 85% of G_t absorption was lost from the membranes, respectively. In a control experiment in which suramin was replaced by 3-kDa heparin no loss of absorption by G_t was observed (Fig. 6, *D* and *E*). In summary, the ATR-FTIR data indicate that suramin exerts its effect on signaling by rhodopsin through a loss of membrane affinity of G_t rather than by affecting the structure of rhodopsin, MII, $MIIG_t$, or occupation of the GTP-binding site of G_t.

DISCUSSION

The influence of suramin on coupling of G_t to rhodopsin

We have demonstrated that pharmacologically relevant concentrations of suramin affect activation of G_t by bovine rhodopsin. This has made possible an analysis of the mechanism by which suramin acts on G-protein signaling in a well characterized in vitro model system. Kinetic analyses of G_t activation demonstrate that suramin affects coupling of G_t to MII but alters neither the rate of nucleotide uptake nor GTP hydrolysis. Likewise, neither the MI/MII equilibrium nor the structure of rhodopsin and $MIIG_t$ is altered by suramin at concentrations that abolish G_t activation. Instead, the rate of association of G_t with MII is reduced.

$MIIG_t$ formation exhibits a fast component attributable to efficient collisions between MII and membrane-bound G_t and a slow component for the transition of G_t from a free to a disk-membrane-bound form (Schleicher and Hofmann, 1987). As membrane association is the rate-limiting step, the influence of suramin can be explained by inhibition of G_t binding to photoactivated disk membranes. The molecular processes underlying this transition may be very similar to or identical with those during association of G_t with membranes in the dark. Thus, suramin-induced dissociation of G_t from disk membranes in the dark, evidenced by ATR-FTIR, may be directly related to the mechanism by which $MIIG_t$ formation is impaired under conditions of multiple activation cycles. Because membrane anchoring of G_t is mediated by $G_{t\alpha}$ (Seitz et al., 1999), it is likely that suramin perturbs the membrane attachment site on $G_{t\alpha}$. Binding of suramin to $G_{t\alpha}$ is evidenced by FRET and is characterized by a K_d of $\sim$0.5 μM. The evaluation of G_t activation rates is in general agreement with this K_d. Even in the realm of a simplified reaction model, including only GTP uptake and hydrolysis, half-maximal inhibition occurred at 6 μM suramin, whereas 3 μM would be expected from the estimated K_d of 0.5 μM (conditions of the experiment shown in Fig. 1). In a more realistic three-step model, 50% reduction of the rate constant for $MIIG_t$ complex formation was observed at 2.5 μM suramin concentration. This agrees precisely with 50% saturation of suramin-binding sites with a K_d of $\sim$0.5 μM (conditions of the experiment shown in Fig. 2) and strongly suggests that suramin binds in a 1:1 stoichiometry to $G_{t\alpha}$ as reported for binding to $G_{s\alpha}$ (Hohenegger et al., 1998). Half-maximal dissociation of G_t from disk membranes measured by ATR-FTIR spectroscopy occurred at higher suramin concentration (10–20 μM). Taking into account the different experimental conditions, the concentrations for half-maximal effects of suramin in both assays appear to be very similar. Therefore, our data suggest that 1) occupation of a single suramin-binding site on $G_{t\alpha}$ with K_d of $\sim$0.5 μM is the predominant cause for the inhibition of rhodopsin-catalyzed G_t activation, and 2) the rate of complex formation between suramin-bound G_t and MII is specifically impaired by a reduced affinity of suramin-bound $G_{t\alpha}$ for photoreceptor membranes.

Reduction of membrane affinity of $G_{t\alpha}$ by suramin may involve electrostatic repulsion of suramin-bound $G_{t\alpha}$ (carrying six negative extra charges) from disk membranes and/or interference with the exposure of the N-terminal acyl chains. Results from SDS-PAGE of supernatants of G_t-containing solutions (3 μM) equilibrated in the dark with disk membranes agree with a reduced membrane affinity of G_t in the presence of suramin (data not shown). The same holds for binding of G_t to electrically neutral phosphatidylcholine vesicles, rendering likely a specific effect on lipid anchoring. The topology of the suramin-binding site on $G_{t\alpha}$ needs further investigation, but one of the two chromophoric 1,3,6-naphthalenetrisulfonate (NTS) moieties may bind near Trp^{207}. This is suggested by the suramin-dependent reduction of nucleotide-induced fluorescence changes of $G_{t\alpha}$ known to arise from Trp^{207}. Although binding of suramin to nucleotide-binding sites has been described for other proteins (van Rhee et al., 1994; Khaled et al., 1995), the different elution properties of nucleotides versus suramin (Figs. 5 and 6) and the unaltered rate constant for nucleotide uptake consistently disfavor binding to the nucleotide-binding site of G_t. Electrostatic interactions between NTS and positively charged amino acids have been inferred from the solution structure of NTS-bound acidic fibroblast growth factor (Lozano et al., 1998) and may be crucial for binding of NTS to G_t as well. Preliminary docking simulations using the program FlexX provided by the Gesellschaft für Mathematische Datenanalyse (Bonn, Germany), also resulted in highest-scoring solutions for binding of NTS to $G_{t\alpha}$ (Protein Data Bank entry 1TAD) in positions within less than 3 Å from the positively charged guanidinium groups of Arg^{201} and Arg^{204} and 10–15 Å apart from Trp^{207}. We suspect that the drug approaches the N-terminus of $G_{t\alpha}$ where it may interfere with membrane anchoring (Matsuda et al., 1994; Seitz et al., 1999) and may additionally affect electrostatically driven steps during receptor recognition (Fanelli et al., 1999).

Comparison with the action of suramin on other receptor G-protein tandems

Structural and functional properties are probably conserved among members of each class of GPCRs. Two modes of action of suramin on G_s-, G_i-, and G_o-dependent signaling by class I (rhodopsin-like) GPCRs have been described. One mode is the reduction of basal nucleotide exchange at submicromolar to micromolar concentrations of suramin. We have shown here that suramin binds to $G_{t\alpha}$ in a 1:1 stoichiometry as reported for other G-proteins (Hohenegger et al., 1998) and with a K_d that falls in the same range as the EC_{50} for suppression of basal nucleotide exchange. However, G_t does not exhibit receptor-independent nucleotide exchange. Correspondingly, the rhodopsin G_t model system

was not expected to respond to this particular mode of suramin action. Another mode of suramin action is uncoupling from the receptor (Beindl et al., 1996). We have demonstrated that inhibition of rhodopsin-dependent G_t activation does indeed occur. It has been shown for $G_{s\alpha}$ that suramin binds not only to epitopes involved in receptor recognition but also overlaps with effector binding sites (Freissmuth et al., 1996). Trp^{207} in $G_{t\alpha}$ is near switch II of $G_{t\alpha}$ and thus close to regions that bind to the effector (Berlot and Bourne, 1992; Rarick et al., 1992). Binding of suramin to that region would also be consistent with the preferential quenching of fluorescence from Trp^{207}. Finally, binding of suramin to $G_{i\alpha}/G_{s\alpha}$ has been shown to cause dissociation of the ternary complex with agonist-bound receptors (Beindl et al., 1996). Because the agonist of rhodopsin, all-*trans* retinal, is covalently bound, an analogous action of suramin was not expected in this system, and dissociation of $MIIG_t$ was not observed. This parallels the quasi-competitive behavior of suramin with respect to agonist as increasing receptor occupancy could reverse the destabilizing effect of suramin on the ternary complex of ligand-activated receptors.

The action of suramin on signaling by other G-protein α-subunits appears to be paralleled by its action on G_t when the unique features of this system are taken into account. Our data further suggest that inhibition of receptor-catalyzed G-protein activation may operate through a reduced membrane affinity of suramin-bound G-protein α-subunits. Binding to membranes is primarily mediated by G_α-palmitoylation and to a less extent by N-terminal myristoylation (as reviewed in Wedegaertner et al., 1995; Milligan and Grassie, 1997). G_t is not palmitoylated and may be particularly sensitive to destabilization of membrane anchoring via a single N-terminal acylation. However, G-protein palmitoylation is a dynamic process. For example, palmitate turnover on $G_{s\alpha}$ in S49 cells has been shown to become accelerated upon β-adrenergic receptor activation (Wedegaertner and Bourne, 1994). Therefore, the acylation state and, correspondingly, the membrane affinity of other G_α-subunits may transiently correspond with that of G_t.

CONCLUSIONS

Rhodopsin G_t interactions may constitute a versatile in vitro model system to elucidate the action of suramin-related drugs on G-protein-dependent signaling. Furthermore, our results hint at a possible adverse effect on scotopic vision in patients receiving suramin treatment. Constant monitoring of dosage in these patients is important because of toxic effects of suramin. A putative impairment of rhodopsin-mediated dim light vision by suramin needs further investigation as it may correlate with other adverse effects that need to be controlled in clinical studies.

We thank Prof. T. P. Sakmar, in whose lab G.K.A. is a post-doctoral associate. We are also grateful to Prof. K. Vogt who generously provided the laboratory for K.F. at the Institut fuer Biologie I at University Freiburg. Furthermore, introduction to the program FlexX by Dr. G. Metz and excellent technical assistance from B. Mayer is gratefully acknowledged.

This research was supported by Deutsche Forschungsgemeinschaft grant FA 248/4–1 to K.F.

REFERENCES

Antonny, B., A. Otto-Bruc, M. Chabre, and T. M. Vuong. 1993. GTP hydrolysis by purified a-subunit of transducin and its complex with the cyclic GMP phosphodiesterase inhibitor. *Biochemistry.* 32:8646–8653.

Beindl, W., T. Mitterauer, M. Hohenegger, A. P. Ijzerman, C. Nanoff, and M. Freissmuth. 1996. Inhibition of receptor/G protein coupling by suramin analogues. *Mol. Pharmacol.* 50:415–423.

Berlot, C. H., and H. R. Bourne. 1992. Identification of effector-activating residues of $G_{s\alpha}$. *Cell.* 68:911–922.

Birge, R. R., and R. B. Barlow. 1995. On the molecular origins of thermal noise in vertebrate and invertebrate photoreceptors. *Biophys. Chem.* 55:115–126.

Butler, S., E. C. H. Kelly, F. McKenzie, S. Guild, M. O. Wakelam, and G. Milligan. 1988. Differential effects of suramin on the coupling of receptors to individual species of pertussis-toxin-sensitive guanine-nucleotide-binding proteins. *Biochem. J.* 251:201–205.

Chaudhry, V., M. A. Eisenberger, V. J. Sinibaldi, K. Sheikh, J. W. Griffin, and D. R. Cornblath. 1996. A prospective study of suramin-induced peripheral neuropathy. *Brain.* 119:2039–2052.

Coffey, R. J., Jr., E. B. Leof, G. D. Shipley, and H. L. Moses. 1987. Suramin inhibition of growth factor receptor binding and mitogenicity in AKR-2B cells. *J. Cell. Physiol.* 132:143–148.

Dawson, N., W. D. Figg, O. W. Brawley, R. Bergan, M. R. Cooper, A. Senderowicz, D. Headlee, S. M. Steinberg, M. Sutherland, N. Patronas, E. Sausville, W. M. Linehan, E. Reed, and O. Sartor. 1998. Phase II study of suramin plus aminoglutethimide in two cohorts of patients with androgen-independent prostate cancer: simultaneous antiandrogen withdrawal and prior antiandrogen withdrawal. *Clin. Cancer Res.* 4:37–44.

Dreicer, R., D. C. Smith, R. D. Williams, and W. A. See. 1999. Phase II trial of suramin in patients with metastatic renal cell carcinoma. *Invest. New Drugs.* 17:183–186.

Ernst, O. P., C. Bieri, H. Vogel, and K. P. Hofmann. 2000. Intrinsic biophysical monitors of transducin activation: fluorescence, UV-visible spectroscopy, light scattering, and evanescent field techniques. *Methods Enzymol.* 315:471–489.

Fahmy, K. 1998. Binding of transducin and transducin-derived peptides to rhodopsin studied by attenuated total reflection-Fourier transform infrared difference spectroscopy. *Biophys. J.* 75:1306–1318.

Fahmy, K., F. Jäger, M. Beck, T. A. Zvyaga, and T. P. Sakmar. 1993. Protonation states of membrane-embedded carboxylic acid groups in rhodopsin and metarhodopsin II: a Fourier-transform infrared spectroscopic study of site-directed mutants. *Proc. Natl. Acad. Sci. U.S.A.* 90:10206–10210.

Fahmy, K., and T. P. Sakmar. 1993. Light-dependent transducin activation by an ultraviolet-absorbing rhodopsin mutant. *Biochemistry.* 32: 9165–9171.

Fahmy, K., F. Siebert, and T. P. Sakmar. 1994. A mutant rhodopsin with a protonated Schiff base displays an active-state conformation: a Fourier transform infrared spectroscopy study. *Biochemistry.* 33:13700–13705.

Fanelli, F., C. Menziani, A. Scheer, S. Cotecchia, and P. G. De Benedetti. 1999. Theoretical study of the electrostatically driven step of receptor-G-protein recognition. *Proteins.* 37:145–156.

Farrens, D. L., C. Altenbach, K. Yang, W. L. Hubbell, and H. G. Khorana. 1996. Requirement of rigid-body motion of transmembrane helices for light activation of rhodopsin. *Science.* 274:768–770.

Faurobert, E., A. Otto-Bruc, P. Chardin, and M. Chabre. 1993. Tryptophan W207 in transducin T alpha is the fluorescence sensor of the G protein activation switch and is involved in the effector binding. *EMBO J.* 12:4191–4198.

Firsching, A., P. Nickel, P. Mora, and B. Allolio. 1995. Antiproliferative and angiostatic activity of suramin analogues. *Cancer Res.* 55: 4957–4961.

Freissmuth, M., S. Boehm, W. Beindl, P. Nickel, A. P. Ijzerman, M. Hohenegger, and C. Nanoff. 1996. Suramin analogues as subtype-selective g protein inhibitors. *Mol. Pharmacol.* 49:602–611.

Fung, B. K.-K., J. B. Hurley, and L. Stryer. 1981. Flow of information in the light-triggered cyclic nucleotide cascade of vision. *Proc. Natl. Acad. Sci. U.S.A.* 75:152–156.

Gagliardi, A. R., M. Kassack, A. Kreimeyer, G. Muller, P. Nickel, and D. C. Collins. 1998. Antiangiogenic and antiproliferative activity of suramin analogues. *Cancer Chemother. Pharmacol.* 41:117–124.

Gether, U. 2000. Uncovering molecular mechanisms involved in activation of G protein-coupled receptors. *Endocr. Rev.* 21:90–113.

Han, M., S. W. Lin, M. Minkova, S. O. Smith, and T. P. Sakmar. 1996. Functional interaction of transmembrane helices 3 and 6 in rhodopsin: replacement of phenylalanine 261 by alanine causes reversion of phenotype of a glycine 121 replacement mutant. *J. Biol. Chem.* 271: 32337–32342.

Helmreich, E. J., and K. P. Hofmann. 1996. Structure and function of proteins in G-protein-coupled signal transfer. *Biochim. Biophys. Acta.* 1286:285–322.

Hemady, R. K., V. J. Sinibaldi, and M. A. Eisenberger. 1996. Ocular symptoms and signs associated with suramin sodium treatment for metastatic cancer of the prostate. *Am. J. Ophthalmol.* 121:291–296.

Higashijima, T., K. M. Ferguson, P. C. Sternweis, E. M. Ross, M. D. Smigel, and A. G. Gilman. 1987. The effect of activating ligands on the intrinsic fluorescence of guanine nucleotide-binding regulatory proteins. *J. Biol. Chem.* 262:752–756.

Hohenegger, M., M. Waldhoer, W. Beindl, B. Böing, A. Kreimeyer, P. Nickel, C. Nanoff, and M. Freissmuth. 1998. $G_{s\alpha}$-selective G protein antagonists. *Proc. Natl. Acad. Sci. U.S.A.* 95:346–351.

Höller, C., M. Freissmuth, and C. Nanoff. 1999. G proteins as drug targets. *Cell. Mol. Life Sci.* 55:257–270.

Huang, R. R. C., R. N. Dehaven, A. H. Cheung, R. E. Diehl, R. A. F. Dixon, and C. D. Strader. 1990. Identification of allosteric antagonists of receptor guanine nucleotide-binding protein interactions. *Mol. Pharmacol.* 37:304–310.

Jäger, F., K. Fahmy, T. P. Sakmar, and F. Siebert. 1994. Identification of glutamic acid 113 as the Schiff base proton acceptor in the metarhodopsin II photointermediate of rhodopsin. *Biochemistry.* 33:10878–10882.

Ji, T. H., M. Grossmann, and I. Ji. 1998. G protein-coupled receptors. I. Diversity of receptor-ligand interactions. *J. Biol. Chem.* 273: 17299–17302.

Khaled, Z., D. Rideout, K. R. O'Driscoll, D. Petrylak, A. Cacace, R. Patel, L. C. Chiang, S. Rotenberg, and C. A. Stein. 1995. Effects of suramin-related and other clinically therapeutic polyanions on protein kinase C activity. *Clin. Cancer Res.* 1:113–122.

Kühn, H. 1980. Light- and GTP-regulated interaction of GTPase and other proteins with bovine photoreceptor membranes. *Nature.* 283:587–589.

Lozano, R. M., M. Jimenez, J. Santoro, M. Rico, and G. Gimenez-Gallego. 1998. Solution structure of acidic fibroblast growth factor bound to 1,3,6-naphthalenetrisulfonate: a minimal model for the anti-tumoral action of suramins and suradistas. *J. Mol. Biol.* 281:899–915.

Matsuda, T., T. Takao, Y. Shimonishi, M. Murata, T. Asano, and T. X. Yoshizawa. 1994. Characterization of interactions between transducin alpha/beta gamma-subunits and lipid membranes. *J. Biol. Chem.* 269: 30358–30363.

Mély, Y., M. Cadène, I. Sylte, and J. G. Bieth. 1997. Mapping the suramin-binding sites of human neutrophil elastase: investigation by fluorescence resonance energy transfer and molecular modeling. *Biochemistry.* 36:15624–15631.

Menon, S. T., M. Han, and T. P. Sakmar. 2001. Rhodopsin: the structural basis of molecular physiology. *Physiol. Rev.* 81:1659–1688.

Milligan, G., and M. A. Grassie. 1997. How do G-proteins stay at the plasma membrane? *Essays Biochem.* 32:49–60.

Mirza, M. R., E. Jakobsen, P. Pfeiffer, B. Lindebjerg-Clasen, J. Bergh, and C. Rose. 1997. Suramin in non-small cell lung cancer and advanced breast cancer: two parallel phase II studies. *Acta Oncol.* 36:171–174.

Okada, T., O. P. Ernst, K. Palczewski, and K. Hofmann. 2001. Activation of rhodopsin: new insights from structural and biochemical studies. *Trends Biochem. Sci.* 26:318–324.

Oseroff, A. R., and R. H. Callender. 1974. Resonance Raman spectroscopy of rhodopsin in disk membranes. *Biochemistry.* 13:4243–4248.

Otto-Bruc, A., B. Antonny, and T. M. Vuong. 1994. Modulation of the GTPase activity of transducin: kinetic studies of reconstituted systems. *Biochemistry.* 33:15215–15222.

Palczewski, K., T. Kumasaka, T. Hori, C. A. Behnke, H. Motoshima, B. A. Fox, Le, I. Trong, D. C. Teller, T. Okada, R. E. Stenkamp, M. Yamamoto, and M. Miyano. 2000. Crystal structure of rhodopsin: a G protein-coupled receptor. *Science.* 289:739–745.

Papermaster, D. S. 1982. Preparation of rod outer segments. *Methods Enzymol.* 81:48–52.

Pigault, C., and D. Gérard. 1984. Influence of the location of tryptophanyl residues in proteins on their photosensitivity. *Photochem. Photobiol.* 40:291–296.

Rarick, H. M., N. O. Artemyev, and H. E. Hamm. 1992. A site on rod G protein alpha subunit that mediates effector activation. *Science.* 256: 1031–1033.

Rath, P., L. L. J. DeCaluwé, P. H. M. Boovee-Geurts, W. J. DeGrip, and K. J. Rothschild. 1993. Fourier transform infrared difference spectroscopy of rhodopsin mutants: light activation of rhodopsin causes hydrogen-bonding change in residue aspartic acid-83 during meta II formation. *Biochemistry.* 32:10277–10282.

Rieke, F., and D. A. Baylor. 1996. Molecular origin of continuous dark noise in rod photoreceptors. *Biophys. J.* 71:2553–2572.

Schleicher, A., and K. P. Hofmann. 1987. Kinetic study on the equilibrium between membrane-bound and free photoreceptor G-protein: membrane association of G-protein. *J. Membr. Biol.* 95:271–281.

Seitz, H. R., M. Heck, K. P. Hofmann, T. Alt, J. Pellaud, and A. Seelig. 1999. Molecular determinants of the reversible membrane anchorage of the G-protein transducin. *Biochemistry.* 38:7950–7960.

Sheikh, S. P., T. A. Zvyaga, O. Lichtarge, T. P. Sakmar, and H. R. Bourne. 1996. Rhodopsin activation blocked by metal-ion-binding sites linking transmembrane helices c and f. *Nature.* 383:347–350.

Shichi, H., K. Yamamoto, and R. L. Somers. 1984. GTP binding protein: properties and lack of activation by phosphorylated rhodopsin. *Vision Res.* 24:1523–1531.

Siebert, F. 1995. Application of FTIR spectroscopy to the investigation of dark structures and photoreactions of visual pigments. *Israel J. Chem.* 35:309–323.

van Rhee, A. M., M. P. van der Heijden, M. W. Beukers, A. P. Ijzerman, W. Soudijn, and P. Nickel. 1994. Novel competitive antagonists for P2 purinoceptors. *Eur. J. Pharmacol.* 268:1–7.

Waldhoer, M., E. Bofill-Cardona, G. Milligan, M. Freissmuth, and C. Nanoff. 1998. Differential uncoupling of A1 adenosine and D2 dopamine receptors by suramin and didemethylated suramin (NF037). *Mol. Pharmacol.* 53:808–818.

Wedegaertner, P. B., and H. R. Bourne. 1994. Activation and depalmitoylation of $G_{s\alpha}$. *Cell.* 77:1063–1070.

Wedegaertner, P. B., P. T. Wilson, and H. R. Bourne. 1995. Lipid modifications of trimeric G proteins. *J. Biol. Chem.* 270:503–506.

Yamanaka, G., F. Eckstein, and L. Stryer. 1985. Stereochemistry of the guanyl nucleotide binding site of transducin probed by phosphorothioate analogues of GTP and GDP. *Biochemistry.* 24:8094–8101.

Zhang, Y. L., Y. F. Keng, Y. Zhao, L. Wu, and Z. Y. Zhang. 1998. Suramin is an active site-directed, reversible, and tight-binding inhibitor of protein-tyrosine phosphatases. *J. Biol. Chem.* 273:12281–12287.

Zvyaga, T. A., K. Fahmy, F. Siebert, and T. P. Sakmar. 1996. Characterization of the mutant visual pigment responsible for congenital night blindness: a biochemical and Fourier-transform infrared spectroscopy study. *Biochemistry.* 35:7536–7545.